Scattering of Ice Particles from a Graphite Surface: A Molecular Dynamics Simulation Study

Anna Tomsic,[†] Nikola Marković,[‡] and Jan B. C. Pettersson*,[†]

Department of Chemistry, Atmospheric Science, Göteborg University, SE-412 96 Göteborg, Sweden, and Department of Chemistry and Bioscience, Chalmers University of Technology, SE-412 96 Göteborg, Sweden

Received: April 30, 2003

Large-scale classical trajectory calculations of $(H_2O)_n$, $n \leq 25\,159$, colliding with a graphite surface have been carried out in order to relate the phenomenon of direct scattering to the initial conditions of the collision. The collisions were performed at normal incidence with the incident velocity ranging from 50 to 2000 ms^{-1} and at surface temperatures between 300 and 1400 K. Upon impact, the cluster is deformed elastically (reversibly) and plastically (irreversibly), and if the elastically stored energy is larger than the binding energy between the cluster and the surface, the cluster scatters directly from the surface. The partitioning between elastic and plastic deformation is governed by the initial conditions (cluster temperature, incident velocity, incident cluster size, and surface temperature). At low incident velocities the scattering probability is controlled by adhesion and at high incident velocities by plastic deformation, and the direct scattering is thus confined to a narrow range of incident velocities. The results are in qualitative agreement with recent experimental studies of water clusters scattering from graphite.

I. Introduction

The detailed dynamics of collisions between ice particles or water droplets and surfaces[1−4] are relevant to many fields of application, that is, coating processes, control of surface contamination in industrial processes, spray cooling of hot surfaces, and atmospheric science. When the size of the particle or droplet decreases, its atomic nature becomes more important, and a model in terms of molecular potentials may then provide a better description of the collision than the concepts of continuum fluid dynamics. Interactions between clusters, composed of up to several thousand molecules, and surfaces have been studied with beam techniques and molecular dynamics (MD) simulations. Clusters this large typically have diameters of a few nanometers and approach the macroscopic size range. Cluster beam experiments and MD simulations[5−7] have shown that when nanometer-sized water clusters collide with graphite, large fragments may leave the surface by means of two different mechanisms: evaporation-mediated emission and direct scattering. The evaporation-mediated mechanism is in operation at surface temperatures above 700 K and can be divided into three stages: (i) cluster deformation on surface impact, (ii) cluster heating by the hot surface, and (iii) cluster emission driven by evaporation of monomers and small fragments. The process is very sensitive to the temperature of the surface, as a rapid heating of the cluster is necessary in order to induce the extensive evaporation necessary to propel the cluster away from the surface. In contrast, the direct scattering mechanism is active at a surface temperature as low as 300 K and appears to be less affected by the surface temperature.[5] Classical molecular dynamics (MD) calculations of $(H_2O)_n$, $n \leq 4094$,[5,7,8] scattering from graphite were able to reproduce the characteristics of the evaporation-mediated emission of large fragments and also gave a detailed picture of the dynamics of the process. In these previous simulations, we did not see any clear evidence of direct scattering. However, if the clusters become sufficiently large, their probability to bounce off the surface should increase.[9−14] In the present study, we have performed MD simulations of clusters consisting of up to 25 159 H_2O molecules in order to enable direct scattering and to characterize the transfer of energy between the different degrees of freedom of the collision process. By describing this "macroscopic" process on a molecular level, we attempt to bridge the gap between molecular dynamics and continuum physics.

II. Molecular Dynamics Simulations

The calculations performed in the present study are of the same type as the ones presented in refs 5, 7, and 8, and for a detailed description we refer to these papers. The initial conditions were chosen to resemble the conditions during cluster beam experiments,[6] where large water clusters impinged on a graphite surface at surface temperatures $T_{surface} \leq 1400$ K. In the experiments, the average incident cluster size was $\leq 14\,000$ monomers/cluster, but the distribution extended up to $n > 20\,000$. We have simulated collisions between $(H_2O)_n$ and graphite, where n has been set to 4094, 12 516, and 25 159 to mimic different parts of the incident size distribution in the experiments. The temperature of the surface ranged from 300 K (room temperature) to 1400 K. The incident velocity in the experiments was 1380 ± 30 ms^{-1}, and a typical incident angle θ_i with respect to the surface normal was 70°. This corresponds to a velocity component in the direction parallel to the surface plane of approximately 1300 ms^{-1}. As the graphite surface is relatively flat clusters may glide long distances on the surface. To simulate an actual collision event, which may involve fragmentation of the cluster, would thus require a very large surface and be computationally too demanding. Recent MD simulations[7] have shown that normal incidence of $(H_2O)_{4094}$

* Corresponding author. Tel: +46 31 772 28 28. Fax: +46 31 772 31 07. E-mail: janp@phc.gu.se.
[†] Göteborg University.
[‡] Chalmers University of Technology.

10.1021/jp030557b CCC: $25.00
Published on Web 08/30/2003

provides a good description of the collision dynamics in surface scattering with an incident angle of 70° from graphite. This lack of effect of the incident angle is due to the relatively weak friction forces experienced by the cluster parallel to the surface plane. We have therefore chosen to use normal incidence throughout the present study.

A. Potential Models. Clusters with diameters of 6, 9, and 12 nm, corresponding to the initial numbers of molecules n_i = 4094, 12 516, and 25 159 per cluster, were cut from simulated bulk ice-Ih[15] constructed using a 96-molecule unit cell.[16] The water molecules were rigid, and their interaction was described using the simple point charge (SPC) model of Berendsen et al.,[17] with a modification of the repulsive part of the potential.[7] The water−water interaction was smoothly switched off between R = 9.5 Å and R = 10.0 Å.[15] That this cutoff value was appropriate was controlled by running a test trajectory of $(H_2O)_{4094}$ impacting a 300 K-surface with $v_i = 200$ ms^{-1}, with the cutoff distance set to 12.5 Å. The monitored properties did not differ significantly from the corresponding trajectory run with the standard cutoff value of 10.0 Å. The water clusters were first allowed to relax (using MD simulations) and then gradually cooled by slowly scaling down the molecular velocities until a temperature close to 0 K was obtained. Clusters formed in a supersonic expansion are evaporatively cooled to a temperature of 180 ± 20 K.[18,19] At this temperature, they are metastable to further evaporation on a time scale of tens of microseconds, the typical time scale for cluster beam experiments.[19,20] Clusters of this size are expected to be crystalline showing a cubic structure.[19] The fact that our simulated clusters have hexagonal structure is not expected to have a significant effect on the dynamics. Previous results[7] for $(H_2O)_{4094}$ showed that the geometry at impact, and thus the orientation of the crystal faces, has a negligible effect on the dynamical behavior of the system on the time scales relevant for direct scattering. The heat capacity of ice has been measured down to very low temperatures.[21−23] The temperature dependence between 0 and 250 K can roughly be described with the equation $C_V = 0.144$ JK^{-2} mol^{-1} T, whereas our classical model has an almost constant heat capacity close to 6R ≈ 50 JK^{-1} mol^{-1} in this temperature range. This discrepancy between the classical model and the quantum mechanical reality results in an overestimation of the amount of internal energy exceeding the zero point energy and presumably also in an overestimation of the flexibility of the cluster. Comparisons between classical MD simulations and quantum mechanical calculations of polyethylene and carbon nanotubes[24] claim that the MD simulations yield structures that are too flexible. There are thus quantum mechanical reasons to believe that the classical model underestimates the ability of the cluster to resist deformation. At 180 K, the excess energy for our clusters is approximately 9.5 kJ mol^{-1}, while it is 2.33 kJ mol^{-1} for bulk ice. The latter value is in the classical model reached already at 47 K. To examine the sensitivity of the collision process to the internal cluster temperature we chose to thermalize the clusters at temperatures of both 47 and 180 K. The initial internal cluster temperature T_i was therefore first increased from 0 to 47 K through scaling of the molecular velocities. The clusters were then allowed to relax with the temperature scaling switched off for a few picoseconds. The scaling-relaxation cycle was repeated until oscillations in the kinetic and potential energy of the cluster had dampened out. The process was then repeated as T_i was raised from 47 to 180 K.

The graphite crystal model was similar to the one used in our previous studies of CF_3Br, H_2O, Xe, and $(H_2O)_n$ scattering from graphite,[5,7,8,25−27] but the slab was larger. In the present study, we used graphite surfaces that had widths of approximately three times the diameters of the clusters. For collisions involving $(H_2O)_{25\,159}$, one layer of the graphite surface consisted of 35 574 atoms arranged in a hexagonal pattern. The edge of the hexagon was 19 nm corresponding to a distance of 33 nm between parallel sides. The surface consisted of three layers of graphite, and the intralayer interaction was described using Brenner's empirical potential function.[28] The number of layers sufficient to adequately describe the dynamics was tested by running trajectories of $(H_2O)_{4094}$ colliding with a surface consisting of five layers at velocities up to 1000 ms^{-1}. These trajectories did not differ significantly from the trajectories run using a three-layer surface. The required minimum surface thickness is determined by the ratio between the momentum of the cluster and its cross section, and three layers should suffice also when the clusters are larger, at least for incident velocities ≤ 470 ms^{-1}. Periodic boundary conditions were applied in the x and y directions, that is, in the surface plane. The periodicity refers to the surface atoms only—the water molecules interact with a finite slab.[7] The interlayer forces were modeled using Morse functions.[25] The bottom layer atoms were fixed in their equilibrium positions, giving a total of 71 148 "dynamic" and 35 574 fixed atoms. The equations of motion for the atoms in contact with the fixed bottom layer were modified by adding stochastic and friction forces[29] in order to simulate the flux of energy between the top of the crystal and the bulk. In addition, each sheet was surrounded by such "stochastic" atoms. Without these "stochastic" atoms the top layer of the crystal cools considerably during cluster impact which is unphysical.

The water−carbon potential used was identical to gas−solid potential no. 4 from ref 26, which performed well in simulations of water monomer scattering. This potential includes Lennard-Jones terms acting between pairs of atoms (O−C, H−C) supplemented by electrostatic contributions from the interaction between the point charges on oxygen and hydrogen atoms in the SPC model and point quadrupoles on the carbon atoms. A switching function similar to the one used for the water−water potential was used to truncate the interaction when the center of mass of a water molecule was 10 Å from a carbon atom. The resulting binding energy of a water molecule to a 0 K graphite surface using this model was 149 meV.

B. Scattering Calculations. The cluster was placed with all molecules outside the range of the water−carbon potential and with the incident velocity vector directed along the surface normal. The results are rather insensitive to the initial orientation of the cluster.[7] In particular this is true for the initial phase of the collision which is of importance for the direct scattering mechanism. We have therefore used the same initial orientation for all trajectories. The classical equations of motion for the carbon atoms and water molecules were integrated using a modified version of the Verlet algorithm[15,30] and a time step of 0.5 fs.[7] Two molecules were considered to belong to the same fragment if their center-of-mass separation was less than the potential cutoff value (10 Å was the standard value in the present case). The number of molecules in the largest fragment, $n_{cluster}$, was calculated along with the perpendicular distance from its center of mass to the surface, $Z_{cluster}$. The instantaneous rotational energy of the cluster was calculated as

$$E_{rot} = {}^1/_2\omega\cdot\boldsymbol{L} \qquad (1)$$

where $\boldsymbol{L}$ is the angular momentum with respect to the center of mass of the fragment and ω is the corresponding angular velocity calculated using the instantaneous moment of inertia

tensor, ***I***. The kinetic energy of the center-of-mass motion of the cluster was calculated as

$$E_{CM} = {}^1/_2 n_{cluster} \cdot m_{H_2O} \cdot v^2 + E_{rot} \quad (2)$$

where m_{H2O} is the mass of one water molecule and v is the velocity of the center-of-mass of the cluster. As we have used nonrotating clusters impacting at normal incidence, most of E_{CM} is found in translation in the direction normal to the surface plane. The translational energy of the water molecules with respect to the center of mass of the cluster and the molecular rotations were summed up to yield E_{kin}, the internal kinetic energy of the cluster. The internal potential energy of the cluster E_{pot}, that is, the water−water-interaction, was also monitored as was the total interaction energy between the water molecules and the graphite surface, $V(H_2O-C)$. As our focus is on the transfer of energy between these different degrees of freedom, energy changes ΔE are usually reported

$$\Delta E = E - E_{initial} \quad (3)$$

where E is the specified energy at time t and $E_{initial}$ is the value of the specified energy at $t = 0$.

III. Results and Discussion

Molecular dynamics simulations have been carried out for initial cluster sizes $n_i = 4094$, 12 516, and 25 159, $T_i = 0$, 47, and 180 K, $T_{surface} = 300$, 700, 1100, and 1400 K, and incident velocities v_i ranging from 50 to 2000 ms^{-1}. The incident velocities in the range 50−1000 ms^{-1} correspond to the normal component of the experimental incident velocity for $44° \leq \theta_i \leq 88°$.[6] $v_i = 2000$ ms^{-1} has no experimental counterpart, the total incident experimental velocity being 1380 ± 30 ms^{-1}. The trajectories were terminated either when the cluster was well outside the range of the water−carbon potential or when it was clear from the $Z_{cluster}$-data that the cluster would not undergo direct scattering. Information regarding initial conditions and the outcome (direct scattering or not) of the trajectories is found in Table 1. To facilitate comparison between different initial conditions, results are reported as functions of a dimensionless time, t_{red}, obtained in the following manner: The time it would take for the center of mass of a cluster with the initial radius r_i to travel from its initial position Z_{start} to a distance equal to r_i from the surface, with a constant velocity equal to v_i, was subtracted from the original time t to yield a corrected time t_{corr}

$$t_{corr} = t - (Z_{start} - r_i)/v_i \quad (4)$$

The normalization time t_{norm} for the system[31]

$$t_{norm} = r_i/v_i \quad (5)$$

was calculated, and our dimensionless time t_{red} was finally computed as

$$t_{red} = t_{corr}/t_{norm} \quad (6)$$

To visualize the degree of compression of the cluster upon impact, $Z_{cluster}$ was divided by the initial cluster radius r_i. By these measures, we eliminate effects on the $Z_{cluster}$-plots that are directly related to the cluster size and velocity.

At impact the cluster is deformed and is temporarily bound to the surface. Figure 1 shows snapshots of $(H_2O)_{12\,516}$ at impact on a 300 K surface for different incident velocities. The snapshots are from at or near the time of the trajectory when the cluster velocity for the first time approaches zero. For clarity, only the oxygen atoms in the water molecules are shown. The degree of compression increases with increasing velocity and at $v_i \geq 1000$ ms^{-1}, the cluster assumes a hat-like shape and spreads out on the surface (Figure 1d). The crystalline structure

TABLE 1: Some Conditions for the $(H_2O)_n$-Graphite Trajectories[a]

$T_{surface}$ (K)	T_i (K)	v_i (ms^{-1})	t_f (ps)	n_f/n_i	$\lvert v_f/v_i \rvert$	direct scattering?
		$n_i = 4094$				
300	0	150	30	1		no
300	0	200	20	1		no
300	0	470	20	1		no
		$n_i = 12\,516$				
300	0	200	25	1	0.53	yes
300	0	470	16	1		no
300	47	50	50	1		no
300	47	100	35	1		no
300	47	200	30	1	0.31	yes
300	47	470	20	1		no
300	47	1000	10	1		no
300	180	200	22	1		no
700	47	200	25	1		no
1100	47	200	25	1		no
1400[b]	47	200	230	0.51	0.21	no
		$n_i = 25\,159$				
300	0	100	43	1		no
300	0	200	31	1	0.45	yes
300	0	470	20	1		no
300	0	1000	30	1		no
300	0	2000	12	0.92		no
300	47	100	40	1		no
300	47	200	30	1	0.38	yes
300	47	470	20	1		no
300	47	1000	15	1		no
1400	47	200	130	0.96		no

[a] The surface temperature and the initial cluster temperature are denoted $T_{surface}$ and T_i respectively; v_i is the initial cluster velocity in the normal direction; t_f is the propagation time; n_f/n_i is the fraction of molecules left in the final cluster fragment; and $|v_f/v_i|$ is the relation between the final and initial velocities in the normal direction. [b] Eventually, this trajectory ended in emission of a large cluster fragment according to the evaporation-mediated mechanism described in refs 5−8 and 40. v_f refers to the final velocity the largest cluster fragment acquired after interacting with the surface according to this mechanism.

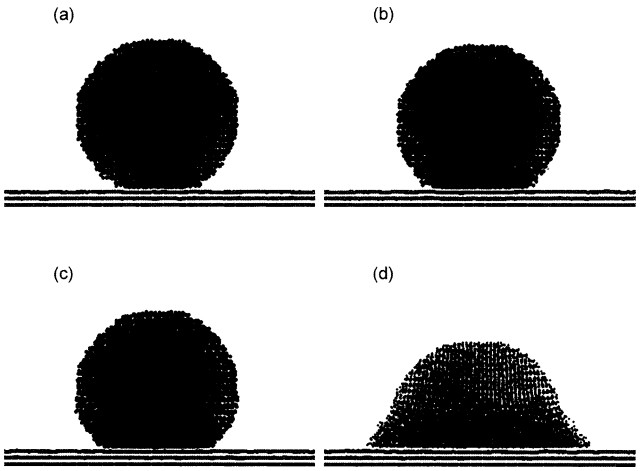

Figure 1. Snapshots at impact from trajectories where $(H_2O)_{12\,516}$ collides with a graphite surface kept at 300 K. Only part of the surface is shown. The initial cluster temperature was 47 K. (a) $v_i = 50$ ms^{-1}, $t = 25$ ps ($t_{red} = 0.041$); (b) $v_i = 200$ ms^{-1}, $t = 10$ ps ($t_{red} = 0.23$); (c) $v_i = 470$ ms^{-1}, $t = 5$ ps ($t_{red} = 0.28$); and (d) $v_i = 1000$ ms^{-1}, $t = 5$ ps ($t_{red} = 0.87$).

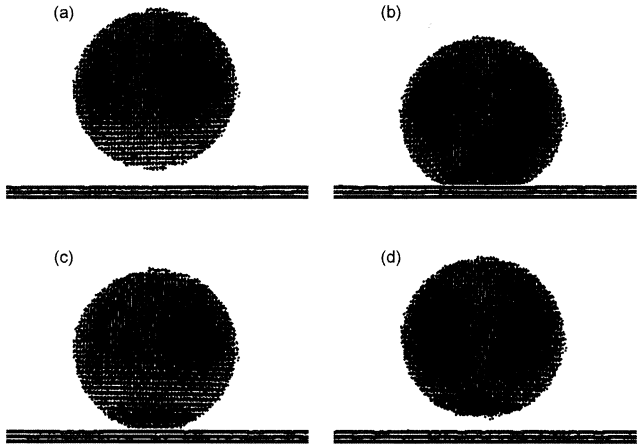

Figure 2. Snapshots from a $(H_2O)_{25\,159}$/graphite trajectory. The incident velocity was 200 ms^{-1} in the normal direction, the initial cluster temperature was 47 K, and the surface temperature 300 K. Only part of the graphite surface is shown. (a) $t = 0$ ($t_{red} = -0.18$); (b) $t = 10$ ps ($t_{red} = 0.18$); (c) $t = 20$ ps ($t_{red} = 0.53$); and (d) $t = 30$ ps ($t_{red} = 0.88$).

in the upper part of the cluster remains undistorted for $v_i \leq 470$ ms^{-1}. At higher velocities, some distortion occurs. The typical propagation time for a trajectory where direct scattering was observed was ~30 ps, and during this time interval no fragmentation of the clusters took place, except for the extreme case of $v_i = 2000$ ms^{-1} where monomers started to leave the cluster in an evaporative fashion after 2.6 ps ($t_{red} = 0.73$). No ejection of fast monomers in the direction parallel to the surface was observed.[32] Direct scattering is thus not associated with fragmentation of the cluster. Most trajectories ended with the clusters becoming trapped on the surface, and direct scattering was only observed for $n_i \geq 12516$, $T_i \leq 47$ K, $T_{surface} = 300$ K, and $v_i = 200$ ms^{-1}. Snapshots from a trajectory where the cluster undergoes direct scattering are displayed in Figure 2 (only O-atoms are shown). As in Figure 1, the cluster is deformed, and temporarily bound to the surface (Figure 2b). Part of the deformation is elastic (reversible) and is returned to the motion of the center of mass of the cluster, and part is plastic, that is, the associated energy is irreversibly dissipated to the internal degrees of freedom of the cluster. Provided the elastically stored energy is large enough to overcome the binding energy between the cluster and the surface, the cluster will recover (Figure 2c) and leave the surface (Figure 2d). In the following, we will discuss the effects of temperature, size, and velocity of the cluster and of surface temperature on the outcome of the collision, in terms of the partitioning between elastic and plastic deformation.

A. Effect of Initial Internal Cluster Temperature. Data from trajectories where $(H_2O)_{12516}$ collides with a graphite surface at $T_{surface} = 300$ K are shown in Figure 3. The incident velocity was 200 ms^{-1} and $T_i = 0$, 47, and 180 K. When the initial internal cluster temperature was 0 and 47 K, the cluster scattered directly from the surface, but at $T_i = 180$ K it was trapped (Figure 3a). The degree of compression is higher at $T_i = 180$ K than at the lower temperatures (Figure 3a), and the adhesive bond developed between the cluster and the surface is considerably stronger (Figure 3b). In Figure 3c, the change in the potential energy of the H_2O-H_2O interaction ΔE_{pot} during the collision is shown. The potential energy rises as the cluster is deformed and reaches a maximum at $t_{red} \approx 0.25$. For $T_i = 0$ and 47 K, about 40−50% of this deformation is elastic and is recovered at $t_{red} \approx 0.4$, but for the more flexible 180 K-cluster, the deformation is permanent. Previous MD simulations of polyethylene particles on different types of surfaces[33] indicate

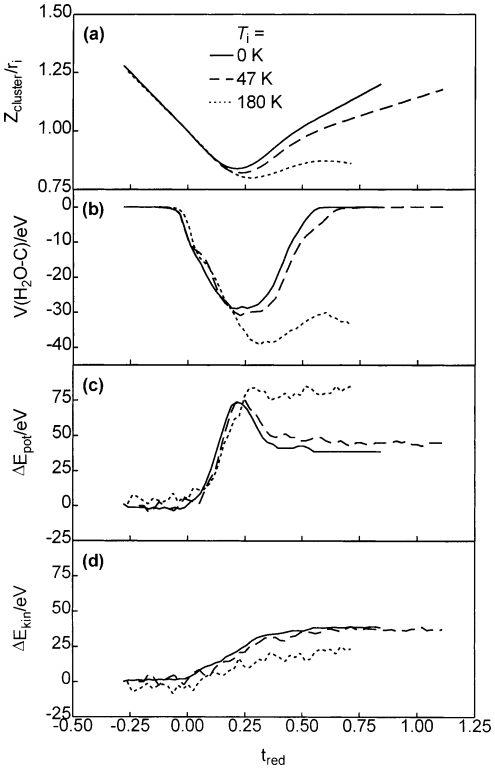

Figure 3. Time dependence of various properties during cluster-surface collisions. Initial conditions: $n_i = 12516$, $T_{surface} = 300$ K, $v_i = 200$ ms^{-1}. The solid lines correspond to $T_i = 0$ K, the dashed lines to $T_i = 47$ K, and the dotted lines to $T_i = 180$ K. (a) The distance from the cluster center of mass to the surface, normalized to the initial cluster radius; (b) the total water−carbon interaction energy; (c) the change in the internal potential energy of the cluster; and (d) the change in the internal kinetic energy of the cluster.

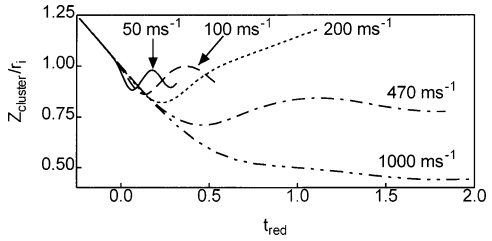

Figure 4. Time dependence of the normalized distance from the cluster center of mass to the surface during cluster-surface collisions. Initial conditions: $n_i = 12\,516$, $T_{surface} = 300$ K, $T_i = 47$ K. The different lines correspond to different incident velocities, as indicated in the figure.

that adhesion and permanent deformation are coupled, in agreement with the present results. The change in the internal kinetic energy of the cluster, ΔE_{kin}, is less steep (Figure 3d), and this energy is permanently dissipated.

B. Effect of Initial Cluster Size and Velocity. Clusters with $n_i = 12\,516$ and 25 159 may scatter directly, but for $n_i = 4094$ no direct scattering was observed. From the results in the previous section follows that the internal cluster temperature should be low in order to facilitate direct scattering. Trajectories with a 4094-cluster at $T_i = 0$ K impacting the surface with different incident velocities were run, but none of them resulted in scattering, demonstrating the difficulty in making a cluster of this size bounce off the surface. As shown in Figure 4, the outcome of the collision is also very sensitive to the incident cluster velocity. For $n_i = 12\,516$ and $T_i = 47$ K, direct scattering is observed only for $v_i = 200$ ms^{-1}. At higher and lower incident velocities, the cluster is trapped. Note that the degree of

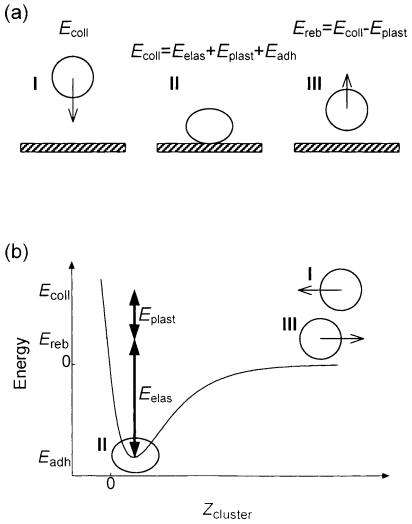

Figure 5. (a) Schematic picture of a collision between a cluster and a surface. (b) Diagram illustrating the transfer of collision energy to the internal degrees of freedom of the cluster.

compression increases with increasing v_i, and that at low v_i the forces acting between the cluster and the surface results in a significant acceleration of the cluster. The size and velocity dependence of the collision outcome can be discussed in terms of a simple energy balance model concerning the repartitioning of the cluster-surface interaction energy and the collision energy upon impact. Figure 5a shows a simplified picture of the collision, and in Figure 5b, a schematic energy diagram is drawn. The collision process can be divided into three stages, referred to in Figure 5 with roman numerals. A cluster impacts on a surface with a collision energy $E_{coll} = n_i m_{H2O} v_i^2/2$ in the direction normal to the surface plane (stage I). Upon impact, it is deformed elastically and plastically, and at some moment it is stationary on the surface (stage II). Neglecting transfer of energy to the surface modes, energy conservation yields that

$$E_{coll} = E_{elas} + E_{plast} + E_{adh} \quad (7)$$

where E_{elas} is the energy stored in elastic deformation of the cluster, E_{plast} corresponds to plastic deformation, and E_{adh} (≤ 0) is the adhesive energy between the cluster and the surface. Rearranging eq 7, we find that the energy available for deformation of the cluster is equal to $E_{coll} - E_{adh}$. The internal energy of the cluster can increase also through transfer of heat from the surface. This energy cannot be recovered after the collision and thus along with E_{plast} contributes to the permanent excitation of the internal degrees of freedom of the cluster. The model is valid even if heat transfer from the surface is present, the only requirement for the validity of the model being that no collision energy is transferred to the surface.

After impact, the elastically stored energy is reconverted into motion of the center of mass of the cluster. If the stored elastic energy is large enough to overcome the adhesion energy, that is

$$E_{elas} \geq |E_{adh}| \quad (8)$$

the cluster may rebound (stage III) with a kinetic energy E_{reb} given by

$$E_{reb} = E_{coll} - E_{plast} \quad (9)$$

Otherwise, it will remain trapped on the surface.

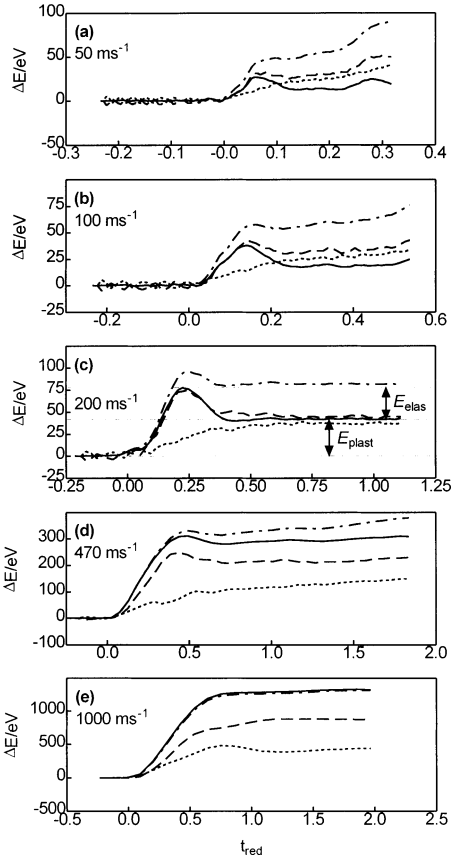

Figure 6. Time dependence of $-(\Delta E_{CM} + V(H_2O-C))$ (solid lines), ΔE_{pot} (dashed lines), ΔE_{kin} (dotted lines), and $\Delta E_{pot} + \Delta E_{kin}$ (dot−dashed lines) during cluster-surface collisions at different incident velocities, indicated in each panel. Initial conditions: $n_i = 12516$, $T_{surface} = 300$ K, and $T_i = 47$ K.

Provided no collision energy is transferred to surface modes, the sum of the change in center-of mass-motion and the water−carbon interaction energy, $\Delta E_{CM} + V(H_2O-C)$, represents the energy loss into internal degrees of freedom of the cluster. For $v_i = 200$ ms^{-1}, the negative of this sum, $-(\Delta E_{CM} + V(H_2O-C))$, follows ΔE_{pot} closely, as illustrated in Figure 6c. This indicates that energy originating from the collisional interaction preferentially is channeled into positional changes of the water molecules in the cluster and that the internal kinetic energy increases mainly due to heat transfer from the surface. For $v_i = 200$ ms^{-1}, the coupling between ΔE_{pot} and $-(\Delta E_{CM} + V(H_2O-C))$ is good at all examined internal cluster temperatures (section IIIA). At lower velocities (Figure 6a,b), $-(\Delta E_{CM} + V(H_2O-C)) < \Delta E_{pot}$, signifying an increase in potential energy caused by heat transfer from the surface. At velocities higher than 200 ms^{-1} (Figure 6d,e), $-(\Delta E_{CM} + V(H_2O-C)) > \Delta E_{pot}$ indicating that collision and adhesion energies are transferred also to the kinetic degrees of freedom of the cluster. Only at $v_i \geq 1000$ ms^{-1} does $-(\Delta E_{CM} + V(H_2O-C))$ exceed the total change in internal cluster energy, and then only with a few percent (Figure 6e). This means that the collision and adhesion energies are efficiently transferred to the cluster, not to the surface. Equation 7 and the assumption that energy transfer to surface modes is negligible is thus applicable in the present case. Note that the peak in ΔE_{pot} disappears as the incident velocity increases and that a small peak in ΔE_{kin} instead starts to appear (Figure 6e), indicating the onset of a "shock wave". This kinetic energy is subsequently redistributed into internal degrees of freedom of the cluster.

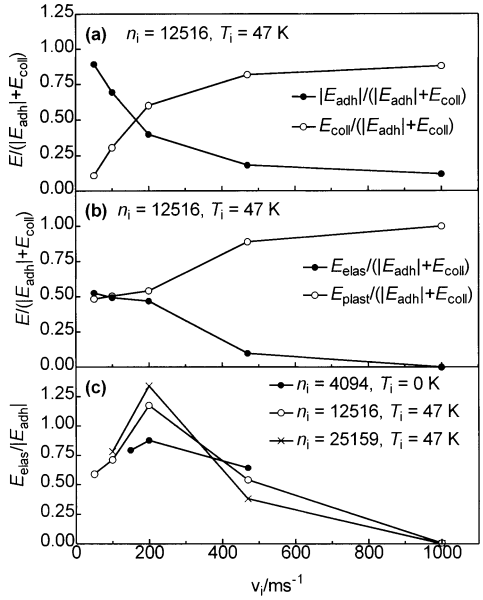

Figure 7. Energies associated with the energy balance model as a function of incident velocity. The initial conditions are indicated in each panel. (a) The relative contribution of the adhesion ($|E_{adh}|$) and collision (E_{coll}) energies to the energy available for deformation of the cluster ($|E_{adh}| + E_{coll}$); (b) the partitioning of $|E_{adh}| + E_{coll}$ between elastic and plastic deformation of the cluster; and (c) the quotient between the elastic deformation and the adhesion energy.

E_{plast} and E_{elas} can be estimated from the plot of $-(\Delta E_{CM} + V(H_2O-C))$ during the collision (Figure 6c). In principle, these energies could also be estimated from the changes in internal cluster energy, but as some heat is transferred from the surface this is difficult. E_{plast} is the value of $-(\Delta E_{CM} + V(H_2O-C))$ evaluated after the passage of the first local maximum in the $-(\Delta E_{CM} + V(H_2O-C))$-curve. E_{elas} is the first local maximum value of $-(\Delta E_{CM} + V(H_2O-C))$ minus E_{plast} (Figure 6c), and E_{adh} is taken to be the first local minimum value of $V(H_2O-C)$, the interaction energy between the water molecules and the graphite surface.

The partitioning of the energy available for cluster deformation is shown in Figure 7. In Figure 7a, the relative contributions of the adhesion and collision energies show that the adhesion energy is very important at low incident velocity but that its importance decreases with increasing v_i. Figure 7b shows the distribution between elastic and plastic deformation. At $v_i >$ 200 ms^{-1}, there is a marked increase in the plastic deformation, and almost all of the available energy is channeled into irreversible deformation of the cluster. At these velocities, $E_{plast} > E_{coll}$ precluding direct scattering. The probability of direct scattering is thus controlled by adhesion at low incident velocities and by plastic deformation at higher incident velocities. For $n_i = 15\,216$, there is only a small "window" of incident velocities where direct scattering is possible, that is, where eq 8 is valid. In Figure 7c it is demonstrated that the stored elastic energy is large enough to overcome the adhesion energy only for $v_i = 200$ ms^{-1}. The limited data from other n_i also plotted in Figure 7c indicate that the ability to overcome adhesion increases with increasing cluster size, in accordance with refs 9−14. For $n_i = 4094$, the maximum of the $E_{elas}/|E_{adh}|$-curve lies below 1, that is, it is impossible to achieve direct scattering with a cluster as small as $(H_2O)_{4094}$.

Good correlation between macroscopic models and MD simulations was previously achieved in a study of $(H_2O)_n-(H_2O)_n$-collisions, with $n = 125$ and 1000.[34] Collisions between micrometer-sized solid particles and surfaces have been studied

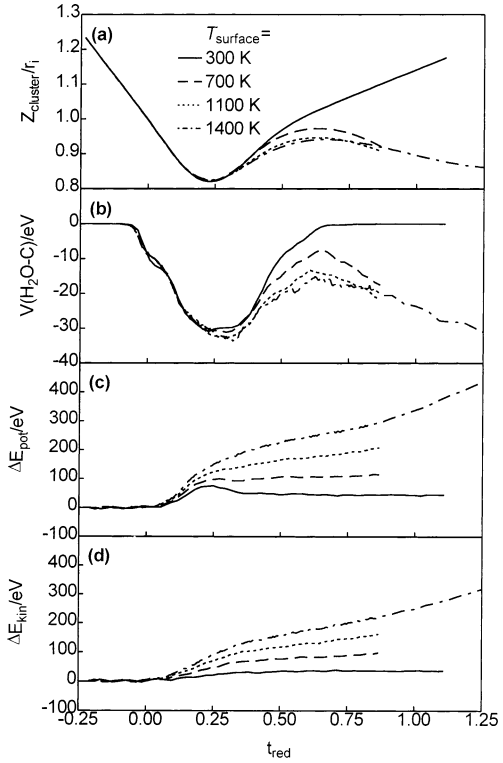

Figure 8. Time dependence of various properties during cluster-surface collisions. Initial conditions: $n_i = 12516$, $T_i = 47$ K, $v_i = 200$ ms^{-1}. The different lines correspond to different surface temperatures, as indicated in 8 part a. (a) The normalized distance from the cluster center of mass to the surface; (b) the total water−carbon interaction energy; (c) the change in the internal potential energy of the cluster; and (d) the change in the internal kinetic energy of the cluster.

experimentally and by means of numerical models.[9−14,35,36] These studies have focused on the low-velocity limit for direct scattering, that is, the critical velocity where adhesion is overcome by the energy stored in elastic deformation. Particles with diameters around 10 μm have critical velocities in the order of 0.1−1 ms^{-1}.[14] Assuming that this critical velocity is inversely proportional to the particle diameter,[11] particles with diameters around 10 nm should overcome adhesion at incident velocities of 100−1000 ms^{-1}. A large decrease in the quotient between rebound velocity and incident velocity due to plastic deformation has been reported for micrometer-sized particles,[14,35] but trapping as the incident velocity increases has to our knowledge not been studied in detail. The behavior we observe at high v_i can be related to a transition of the cluster from solidlike to liquidlike at surface impact. Investigations of liquid droplets impinging on surfaces[3,31,37−39] generally deal with phenomena like spreading and splashing—behaviors that are not examined in detail in the present study. However, the ratio of rebound velocity to incident velocity as a function of incident velocity passes through a maximum in the studies of particle impact and also in a study of water drops bouncing off a superhydrophobic surface,[2] and this phenomenon can be related to our findings.

C. Effect of Surface Temperature. Figure 8a shows that the outcome of the collision event is sensitive to the surface temperature. There are tendencies to rebound at all surface temperatures (Figure 8a). These tendencies grow stronger as the surface temperature decreases, but only at $T_{surface} = 300$ K is direct scattering observed. Above $T_{surface} = 300$ K, heat transfer from the surface is important, and the cluster starts to melt (Figure 8c,d). The melting results in a larger contact area and thereby a stronger binding between the cluster and the surface (Figure 8b). The melting also increases the dissipation

of collision energy. In terms of the energy balance model described in the previous section, the net effect of an increasing surface temperature is that E_{adh} is increased and E_{elas} is decreased, resulting in a lower probability for direct scattering. The trajectory at $T_{surface} = 1400$ K was propagated for 230 ps, and the cluster eventually left the surface according to the evaporation-mediated mechanism.[5−7] One factor that promotes evaporation-mediated emission is good contact between the cluster and the surface—a factor that also counteracts direct scattering. The two scattering mechanisms are thus complementary.

Experimentally, the direct scattering channel was observed also for $T_{surface} > 300$ K.[5] This contradicts the results of the present paper, where our limited amount of trajectories suggests that the probability for direct scattering decreases with increasing surface temperature. The outcome of the collision depends on the quotient $E_{elas}/|E_{adh}|$, which increases with increasing cluster size (Figure 7c). In the experiments, direct scattering is observed for clusters smaller than $n_i = 12\,516$, suggesting that our classical model underestimates the ability of the clusters to deform elastically (see section IIA). It is therefore not unlikely that direct scattering is possible even at surface temperatures over 300 K. At very high surface temperatures both scattering channels may contribute to the flux of large clusters from the surface.

IV. Conclusions

Molecular dynamics simulations of large ($n \leq 25\,159$) water clusters colliding with graphite at normal incidence have shown that the clusters may scatter directly from the surface. Upon impact, the collision energy is transferred to internal degrees of freedom of the cluster. The probability of direct scattering depends on the relation between elastic and plastic deformation of the cluster upon impact and on the relation between the elastic deformation and the adhesive energy between the cluster and the surface. These relations confine the direct scattering to a narrow range of incident velocities, and in our calculations, the only incident velocity where direct scattering was observed was 200 ms^{-1}. For a relatively small cluster with $n_i = 4094$, there appears to be no possibility for direct scattering.

The partitioning between elastic and plastic deformation is sensitive to the internal cluster temperature, T_i. At low temperatures ($T_i \leq 47$ K), deformation is to some extent elastic, while the more flexible cluster at $T_i = 180$ K is permanently deformed and does not scatter. Likewise, the plastic deformation increases if the surface temperature is raised. At surface temperatures above room temperature the cluster starts to melt, which results in an increasing permanent deformation in a similar manner as for increasing T_i. If direct scattering is going to occur, the elastically stored energy has to be large enough to overcome the adhesive energy between the cluster and the surface. Melting and plastic deformation results in an enlarged contact area between the cluster and the surface, and the adhesion becomes stronger. This also counteracts direct scattering, although at $v_i = 200$ ms^{-1} the augmented plastic deformation is the more important factor in reducing the scattering probability. In addition to the direct scattering, large water clusters scatter from graphite by evaporation-mediated emission of large fragments. Both scattering channels have been observed and characterized experimentally,[5,6,40] and the evaporation-mediated mechanism has also been successfully modeled by MD simulations.[5,7,8] The direct scattering mechanism has not been simulated until now, and the present study provides detailed knowledge about the dynamics of this type of collision event.

Acknowledgment. This project was supported by the Swedish Research Council.

References and Notes

(1) Bergeron, V.; Bonn, D.; Martin, J. Y.; Vovelle, L. *Nature* **2000**, *405*, 772.
(2) Richard, D.; Quere, D. *Europhys. Lett.* **2000**, *50*, 769.
(3) Pasandideh-Fard, M.; Aziz, S. D.; Chandra, S.; Mostaghimi, J. *Int. J. Heat Fluid Flow* **2001**, *22*, 201.
(4) Aussillous, P.; Quéré, D. *Nature* **2001**, *411*, 924.
(5) Tomsic, A.; Marković, N.; Pettersson, J. B. C. *Chem. Phys. Lett.* **2000**, *329*, 200.
(6) Tomsic, A.; Andersson, P. U.; Marković, N.; Pettersson, J. B. C. *J. Chem. Phys.* **2003**, *119*, 4916.
(7) Tomsic, A.; Andersson, P. U.; Marković, N.; Piskorz, W.; Svanberg, M.; Pettersson, J. B. C. *J. Chem. Phys.* **2001,** *115*, 10509.
(8) Tomsic, A.; Marković, N.; Pettersson, J. B. C. *PCCP* **2001**, *3*, 3667.
(9) Xu, M.; Willeke, K. *J. Aerosol Sci.* **1993**, *24*, 19.
(10) Johnson, K. L.; Pollock, H. M. *J. Adhesion Sci. Technol.* **1994**, *8*, 1323.
(11) Andres, R. P. *Aerosol Sci. Technol.* **1995**, *23*, 40.
(12) Li, X.; Dunn, P. F.; Brach, R. M. *J. Aerosol Sci.* **1999**, *30*, 439.
(13) Brach, R. M.; Dunn, P. F.; Li, X. *J. Adhesion* **2000**, *74*, 227.
(14) John, W. *Aerosol Sci. Technol.* **1995**, *23*, 2.
(15) Bolton, K.; Svanberg, M.; Pettersson, J. B. C. *J. Chem. Phys.* **1999**, *110*, 5380.
(16) Hayward, J. A.; Reimers, J. R. *J. Chem. Phys.* **1997**, *106*, 1518.
(17) Berendsen, H. J. C.; Postma, J. P. M.; van Gunsteren, W. F.; Hermans, J. In *Intermolecular Forces*; Pullman, B., Ed.; Reidel: Dordrecht, 1981; p 331.
(18) Torchet, G.; Schwartz, P.; Farges, J.; de Feraudy, M. F.; Raoult, B. *J. Chem. Phys.* **1983**, *79*, 6196.
(19) Huang, J.; Bartell, L. S. *J. Phys. Chem.* **1995**, *99*, 3924.
(20) Klots, C. E. *J. Chem. Phys.* **1985**, *83*, 5854.
(21) Giauque, W. F.; Stout, J. W. *J. Am. Chem. Soc.* **1936**, *58*, 1144.
(22) Flubacher, P.; Leadbetter, A. J.; Morrison, J. A. *J. Chem. Phys.* **1960**, *33*, 1751.
(23) Sugisaki, M.; Suga, H.; Seki, S. *Bull. Chem. Soc. Jpn.* **1968**, *41*, 2591.
(24) Noid, D. W.; Tuzun, R. E.; Sumpter, B. G. *Nanotechnology* **1997**, *8*, 119.
(25) Någård, M. B.; Markovic, N.; Pettersson, J. B. C. *J. Chem. Phys.* **1998**, *109*, 10350.
(26) Marković, N.; Andersson, P. U.; Någård, M. B.; Pettersson, J. B. C. *Chem. Phys.* **1999**, *247*, 413; *Chem. Phys.* **2000**, *252*, 409 (erratum).
(27) Någård, M. B.; Andersson, P. U.; Marković, N.; Pettersson, J. B. C. *J. Chem. Phys.* **1998**, *109*, 10339.
(28) Brenner, D. W. *Phys. Rev. B* **1990**, *42*, 9458; *Phys. Rev. B* **1992**, 46, 1948 (erratum).
(29) Svanberg, M.; Marković, N.; Pettersson, J. B. C. *Chem. Phys.* **1997**, *220*, 137.
(30) Svanberg, M. *Mol. Phys.* **1997**, *92*, 1085.
(31) Rein, M. *Fluid. Dyn. Res.* **1993**, *12*, 61.
(32) Marković, N.; Pettersson, J. B. C. *J. Chem. Phys.* **1994**, *100*, 3911.
(33) Fukui, K.; Sumpter, B. G.; Runge, K.; Kung, C.-Y.; Barnes, M. D.; Noid, D. W. *Chem. Phys.* **1999**, *244*, 339.
(34) Svanberg, M.; Ming, L.; Marković, N.; Pettersson, J. B. C. *J. Chem. Phys.* **1998**, *108*, 5888.
(35) Dahneke, B. *Aerosol Sci. Technol.* **1995**, *23*, 25.
(36) Rogers, L. N.; Reed, J. *J. Phys. D: Appl. Phys.* **1984**, *17*, 677.
(37) Mundo, C.; Sommerfeld, M.; Tropea, C. *Int. J. Multiphase Flow* **1995**, *21*, 151.
(38) Blake, T. D.; Decamps, C.; De Coninck, J.; de Ruijter, M.; Voué, M. *Colloids Surf. A* **1999**, *154*, 5.
(39) Thoroddsen, S. T.; Sakakibara, J. *Phys. Fluids* **1998**, *10*, 1359.
(40) Andersson, P. U.; Tomsic, A.; Andersson, M. B.; Pettersson, J. B. C. *Chem. Phys. Lett.* **1997**, *279*, 100.